

# Has a thick neutron skin in $^{208}\text{Pb}$ been ruled out?

F. J. Fattoyev<sup>1,\*</sup> and J. Piekarewicz<sup>2,†</sup>

<sup>1</sup>*Department of Physics and Astronomy, Texas A&M University-Commerce, Commerce, TX 75429, USA*

<sup>2</sup>*Department of Physics, Florida State University, Tallahassee, FL 32306, USA*

(Dated: March 22, 2022)

The Lead Radius Experiment (PREX) has provided the first model-independent evidence in favor of a neutron-rich skin in  $^{208}\text{Pb}$ . Although the error bars are large, the reported large central value of 0.33 fm is particularly intriguing. To test whether such a thick neutron-skin in  $^{208}\text{Pb}$  is already incompatible with laboratory experiments or astrophysical observations, we employ relativistic models with neutron-skin thickness in  $^{208}\text{Pb}$  ranging from 0.16 to 0.33 fm to compute ground state properties of finite nuclei, their collective monopole and dipole response, and mass-vs-radius relations for neutron stars. No compelling reason was found to rule out models with large neutron skins in  $^{208}\text{Pb}$  from the set of observables considered in this work.

PACS numbers: 21.10.Gv, 21.60.Jz, 21.65.Ef, 26.60.Kp

The Lead Radius Experiment (“PREX”) at the Jefferson Laboratory has provided the first model-independent evidence on the existence of a neutron-rich skin in  $^{208}\text{Pb}$  [1, 2]. Relying on the fact that the weak charge of the neutron is much larger than the corresponding one in the proton, PREX used parity-violating electron scattering to probe the neutron distribution of  $^{208}\text{Pb}$  [3]. Elastic electron scattering is particularly advantageous as it provides a clean probe of neutron densities that is free from strong-interaction uncertainties. By invoking some mild assumptions, PREX provided the first largely model-independent determination of the neutron radius  $r_n$  of  $^{208}\text{Pb}$ . Since the charge radius—and its corresponding proton radius  $r_p$ —is known with enormous accuracy [4], PREX effectively determined the neutron-skin of  $^{208}\text{Pb}$  to be [1]:  $r_{\text{skin}}^{208} \equiv r_n - r_p = 0.33^{+0.16}_{-0.18}$  fm. While PREX demonstrated excellent control of systematic errors, unforeseen technical problems compromised the statistical accuracy of the measurement. Although such an error is large enough to accommodate the predictions of many theoretical models, its large central value of  $r_{\text{skin}}^{208} = 0.33$  fm is highly intriguing. It is intriguing because most nuclear energy density functionals (EDFs) predict significant lower values [5, 6].

A measurement of the neutron-skin thickness of  $^{208}\text{Pb}$  is of enormous significance due to its very strong correlation to the slope of the symmetry energy around saturation density [5, 7–9]. Given that the slope of the symmetry energy  $L$  is presently poorly known, an accurate measurement of  $r_{\text{skin}}^{208}$  could help constrain the equation of state (EOS) of neutron-rich matter, and thus provide vital guidance in areas as diverse as heavy-ion collisions [10–14] and neutron-star structure [15–20]. Conversely, and precisely because of the enormous reach of  $r_{\text{skin}}^{208}$ , significant constraints on the EOS of neutron-rich matter are starting to emerge as one combines theo-

retical, experimental, and observational information [21]. Indeed, a remarkable consistency seems to appear as one combines laboratory measurements with astrophysical observations [22, 23]. For example, in an analysis of the pygmy dipole resonance in exotic nuclei, Carbone *et al.*, reported values of  $L = (64.8 \pm 15.7)$  MeV and  $r_{\text{skin}}^{208} = (0.196 \pm 0.023)$  fm, finding remarkable overlap with other methods to extract  $L$  [24]. Later on, Steiner and Gandolfi using predictions from Quantum Monte-Carlo simulations for pure neutron matter together with neutron-star observations were able to provide the following stringent limits:  $L = (47.5 \pm 4.5)$  MeV  $\rightarrow r_{\text{skin}}^{208} = (0.171 \pm 0.007)$  fm [25]. Note that the arrow is meant to indicate that the quoted value of  $r_{\text{skin}}^{208}$  is derived from using the strong linear correlation between  $L$  and  $r_{\text{skin}}^{208}$  obtained in Ref. [5]. By improving on the finite-range droplet model, Möller *et al.* were able to determine  $L = (70 \pm 15)$  MeV  $\rightarrow r_{\text{skin}}^{208} = (0.204 \pm 0.022)$  fm, although they recognize that a large variation in  $L$  would not significantly alter the accuracy of their mass model [26]. Finally, two very recent compilations have placed constraints on the density dependence of the symmetry energy from invoking theory, experiment, and observation [22, 23]. In Ref. [22] (where only theoretical and experimental information was used) Tsang *et al.*, obtained constraints of  $L \sim 70$  MeV and  $r_{\text{skin}}^{208} = (0.180 \pm 0.027)$  fm. Meanwhile, Lattimer obtained a value of  $L = (50.5 \pm 9.5)$  MeV  $\rightarrow r_{\text{skin}}^{208} = (0.175 \pm 0.014)$  fm [23]. We reiterate that whereas all these predictions for  $r_{\text{skin}}^{208}$  can be accommodated comfortably within the PREX  $1\sigma$  error, the PREX central value of  $r_{\text{skin}}^{208} = 0.33$  fm is clearly incompatible with all these findings. Besides these recent analyses, many others have been published in the literature. However, we are unaware of any analysis constrained by experimental and observational data that accommodates a large neutron-skin thickness in  $^{208}\text{Pb}$ .

It is the aim of the present contribution to examine critically whether models with large neutron skins are incompatible with both laboratory and astrophysical data. To do so we construct new relativistic density functionals with fairly large values of  $r_{\text{skin}}^{208}$  that are tested against

\*Electronic address: farrooh.fattoyev@tamuc.edu

†Electronic address: jpiekarewicz@fsu.edu

existing data. The relativistic EDFs that will be used are based on the interacting Lagrangian density given in Ref. [27]. Such a Lagrangian density includes a handful of parameters that are calibrated to provide an accurate description of finite nuclei and a Lorentz covariant extrapolation to dense nuclear matter. In addition to some of the standard relativistic EDFs used in the literature, such as NL3 [28, 29], FSUGold [27], and IU-FSU [30], we consider three additional EDFs labeled “TAMUC-FSU” (or “TF” for short) with relatively large neutron skins. Although the parameters of these models do not follow from a strict optimization procedure, a significant effort was made in reproducing some bulk parameters of infinite nuclear matter as well as some critical properties of finite nuclei. However, we note that our work—devoted exclusively to the study of physical observables—ignores powerful theoretical constraints that have emerged from the nearly universal behavior of pure neutron matter at very low densities. Indeed, the models introduced in this work appear inconsistent with such theoretical constraints. Yet, as we show below, it seems that such a shortcoming has no impact on the wide range of physical observables explored in this work. Further details on the behavior of pure neutron matter and the calibration procedure will be provided in a forthcoming publication.

Predictions by the six models described in the text for some bulk parameters of symmetric nuclear matter and of the symmetry energy are displayed in Table I. The notation used for these parameters follows the convention of Ref. [31]. Also displayed are the predictions for the neutron-skin thickness of  $^{208}\text{Pb}$ . As advertised, the TF models all predict fairly large values for  $r_{\text{skin}}^{208}$ , and thus large values for  $L$ . In what follows we examine whether models with such large neutron skins are incompatible with available laboratory or astrophysical data.

We start by displaying in Fig.1 residuals for the binding energy and charge radius of ten magic or semi-magic nuclei: from  $^{16}\text{O}$  to  $^{208}\text{Pb}$ . Experimental data for the binding energies and charge radii were obtained from Refs. [32] and [4], respectively. Note that at present there is no available data for the charge radius of neutron-rich  $^{68}\text{Ni}$  nor for the neutron-deficient  $^{100}\text{Sn}$  [4]. One of the first relativistic EDFs that was accurately calibrated to the ground-state properties of finite nuclei was NL3 [28, 29]. NL3 has been enormously successful in reproducing binding energies and charge radii of nuclei throughout the nuclear chart. However, since the binding energy of stable nuclei is largely an isoscalar property, the relatively large value of  $L$  predicted by NL3 remained untested. Essentially, nuclear binding energies are controlled by the saturation properties of symmetric nuclear matter and the symmetry energy at a density of about two thirds of that of nuclear matter saturation (or  $\simeq 0.1 \text{ fm}^{-3}$ ) [7, 8]; we denote this quantity as  $\bar{J}$ . Thus, as illustrated in Fig.1, NL3 provides a fairly accurate description of the binding energy and charge radius of all

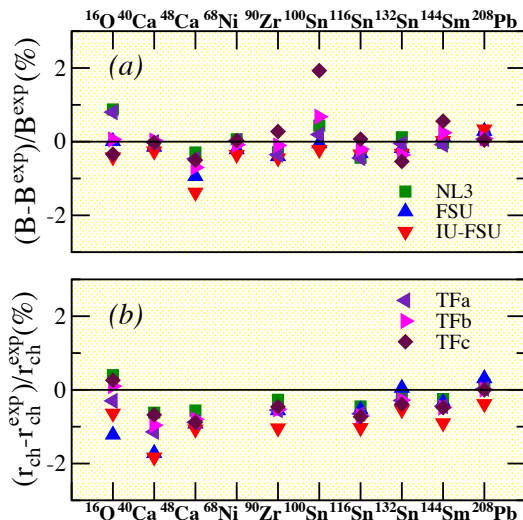


FIG. 1: (Color online) Residuals (in percentage) using the predictions of the six models discussed in the text and experiment (when available) for the binding energy (a) and charge radii (b) of ten magic/semi-magic nuclei across the nuclear chart. Experimental binding energies were obtained from Ref. [32] and charge radii from Ref. [4].

nuclei depicted in the figure. Given that in all models considered in Table I symmetric nuclear matter saturates at about the same place and the value of  $\bar{J}$  differs by no more than  $\sim 15\%$ , we expect an adequate description of binding energies and charge radii for all the models. This assertion is verified in Fig.1. Although only NL3 and FSUGold (or “FSU” for short) have been accurately calibrated, all three TF models provide a description that is consistent with laboratory data. Given that the values of  $L$  tabulated in Table I vary by more than a factor of two between models, we conclude that ground-state masses and charge radii are poor isovector indicators that place no meaningful constraints on the neutron-skin thickness of  $^{208}\text{Pb}$ . This conclusion is in disagreement with the recent findings reported in Ref. [33].

The collective response of finite nuclei provides a far better test of the isovector sector than masses and charge radii. In particular, the monopole response (or “breathing mode”) of neutron-rich nuclei is sensitive to the density dependence of the symmetry energy. Indeed, the incompressibility coefficient of neutron-rich matter, a quantity strongly correlated to the breathing-mode energy, may be written as  $K_0(\alpha) \approx K_0 + (K_{\text{sym}} - 6L + \dots)\alpha^2$ , where  $\alpha \equiv (N - Z)/A$  is the neutron-proton asymmetry [31]. In Fig.2 we display centroid energies for the giant monopole resonance (GMR) in  $^{90}\text{Zr}$ ,  $^{116}\text{Sn}$ ,  $^{144}\text{Sm}$ , and  $^{208}\text{Pb}$  [34–39]. It is important to include nuclei with differing values of  $\alpha$  since the neutron-proton asymmetry provides the lever arm for probing the density dependence of the symmetry energy. For example, whereas NL3—with large values for both  $K_0$  and  $L$ —is consistent with the measured value of the centroid energy in  $^{208}\text{Pb}$

Model	$\rho_0$ (fm $^{-3}$ )	$\varepsilon_0$	$K_0$	$\tilde{J}$	$J$	$L$	$K_{\text{sym}}$	$r_{\text{skin}}^{208}$ (fm)
NL3	0.148	-16.24	271.5	25.68	37.29	118.2	100.9	0.28
FSU	0.148	-16.30	230.0	26.00	32.59	60.5	-51.3	0.21
IU-FSU	0.155	-16.40	231.2	26.00	31.30	47.2	28.7	0.16
TFa	0.149	-16.23	245.1	26.00	35.05	82.5	-68.4	0.25
TFb	0.149	-16.40	250.1	27.59	40.07	122.5	45.8	0.30
TFc	0.148	-16.46	260.5	30.20	43.67	135.2	51.6	0.33

TABLE I: Bulk parameters of infinite nuclear matter at saturation density  $\rho_0$  as predicted by the various models used in the text. The quantities  $\varepsilon_0$  and  $K_0$  represent the binding energy per nucleon and incompressibility coefficient of symmetric nuclear matter, whereas  $J$ ,  $L$ , and  $K_{\text{sym}}$  denote the energy, slope, and curvature of the symmetry energy at  $\rho_0$ ; note that  $\tilde{J}$  represents the value of the symmetry energy at a density of  $\rho \approx 0.103 \text{ fm}^{-3}$ . Also shown are the predictions for the neutron-skin thickness of  $^{208}\text{Pb}$ . All quantities are given in MeV unless otherwise indicated.

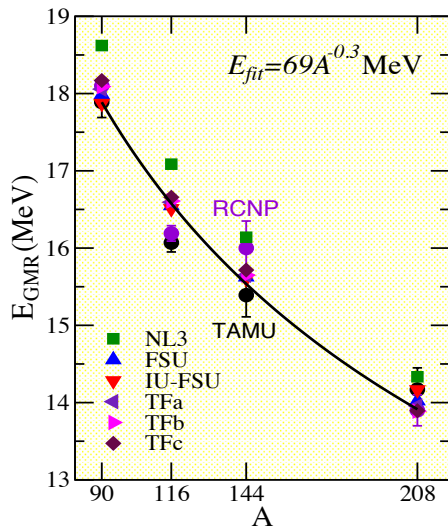


FIG. 2: (Color online) Predictions for the GMR centroid energies of  $^{90}\text{Zr}$ ,  $^{116}\text{Sn}$ ,  $^{144}\text{Sm}$ , and  $^{208}\text{Pb}$  from the six models used in the text. Experimental centroid energies are from Ref. [34] (TAMU) and Refs. [35–39] (RCNP).

( $\alpha = 0.21$ ) it overestimates the centroid energy in  $^{90}\text{Zr}$  ( $\alpha = 0.11$ ). The conception of the FSUGold functional was in large part motivated by the desire to properly describe GMR energies in both  $^{90}\text{Zr}$  and  $^{208}\text{Pb}$  [40]. To do so it was required to soften both the EOS of symmetric matter and the symmetry energy relative to the NL3 predictions [27]. Indeed, with such a softening FSUGold is able to properly describe the experimental GMR energies in all nuclei, except for the case of  $^{116}\text{Sn}$ . Note that the softness of  $^{116}\text{Sn}$  in particular—and of all stable Tin isotopes in general—remains an important open problem [37, 41, 42]. However, what is also evident from the figure is that regardless of the stiffness of the symmetry energy, all models—with the possible exception of NL3—cluster around the FSUGold predictions. This suggests that centroid energies of monopole resonances—even those of nuclei with a large neutron excess—are unable to place stringent constraints on the neutron-skin thickness of  $^{208}\text{Pb}$ .

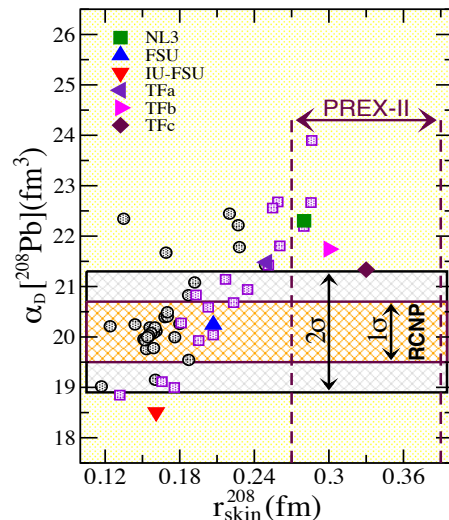


FIG. 3: (Color online) Predictions from 52 nuclear EDFs for the electric dipole polarizability and the neutron-skin thickness of  $^{208}\text{Pb}$ . Constraints on the dipole polarizability from RCNP [43, 44] and from an updated PREX experiment assuming a 0.06 fm error and the same central value [1] have been incorporated into the plot.

In Ref. [45] Reinhard and Nazarewicz demonstrated that the electric dipole polarizability  $\alpha_D$  is a strong isovector indicator that is strongly correlated to the neutron-skin thickness of heavy nuclei. Shortly after, using a large number of EDFs, it was confirmed that such a correlation is robust [6]. The electric dipole polarizability, which is proportional to the inverse energy weighted sum of the isovector dipole response, is a good isovector indicator because the symmetry energy acts as the restoring force. The recent high-resolution measurement of  $\alpha_D$  in  $^{208}\text{Pb}$  at RCNP [43, 44] provides a unique constraint on  $r_{\text{skin}}^{208}$  by ruling out models with either very small ( $r_{\text{skin}}^{208} \lesssim 0.12 \text{ fm}$ ) or very large ( $r_{\text{skin}}^{208} \gtrsim 0.24 \text{ fm}$ ) neutron skins. In this context, the predictions for  $\alpha_D$  from the three stiff TF models is particularly relevant. To test these models against the RCNP data we have directly imported the relevant figure from Ref. [6], supplemented with the predictions from the

IU-FSU and TF models. As alluded earlier and clearly displayed in Fig. 3, the RCNP measurement rules out at the  $1\sigma$  level the predictions of all the models considered in the text—except for FSUGold. It rules out IU-FSU for having too soft a symmetry energy, and NL3 and the three TF models for having one that is too stiff. However, note that the correlation between  $\alpha_D$  and  $r_{\text{skin}}^{208}$  is not linear. Indeed, a far better linear correlation is obtained between  $r_{\text{skin}}^{208}$  and the product of  $J\alpha_D$  [46, 47]. Given the large value of  $J$  suggested by the TFc model, this mitigates the increase of  $\alpha_D$  with  $r_{\text{skin}}^{208}$ , thereby allowing its prediction to be consistent with the RCNP experiment at the  $2\sigma$  level. Finally, note that we have included the projected uncertainty of 0.06 fm for the updated PREX measurement (PREX-II) assuming that its central value of 0.33 fm remains intact. If that proves to be the case, then all 52 models displayed in the figure will be ruled out!

We finish by displaying in Fig. 4 mass-vs-radius relations for neutron stars. Shown with horizontal bars are the two (accurately measured) massive neutron stars of about 2 solar masses reported by Demorest *et al.* [48] and Antoniadis *et al.* [49]. Clearly, theoretical models that predict limiting masses below  $2 M_\odot$  (such as FSUGold) require to stiffen the high-density component of the EOS. Whereas laboratory experiments are of little value in elucidating the maximum neutron-star mass, they play a critical role in constraining stellar radii. This is because the same pressure that pushes against surface tension to create a neutron-rich skin in nuclei pushes against gravity to determine the size of the neutron star. Moreover, although neutron stars contain regions of density significantly higher than those encountered in a nucleus, it has been shown that stellar radii are controlled by the density dependence of the symmetry energy in the immediate vicinity of nuclear-matter saturation density [50]. This provides a powerful “*data-to-data*” relation: The larger the neutron-skin thickness of  $^{208}\text{Pb}$  the larger the radius of a neutron star [16].

Recent advances in X-ray astronomy have allowed for the simultaneous determination of masses and radii of neutron stars. By reaching this important milestone one is now able to pose the following complementary question: how do neutron-star radii constrain the neutron-skin thickness of  $^{208}\text{Pb}$ . The simultaneous determination of stellar masses and radii has emerged from a study of three X-ray bursters by Özel and collaborators [51]. Results from such a study are displayed in Fig. 4 (in the 8 to 10 km region) and suggest very small radii that are difficult to reconcile with the predictions from all models considered in the text, and indeed from most models lacking exotic cores [52]. Shortly after, Steiner, Lattimer, and Brown supplemented Özel’s study with three additional neutron stars and concluded that systematic uncertainties affect the determination of the most probable masses and radii [53]. Their results suggest larger radii of 11 to 12 km and have been depicted in Fig. 4 by the two shaded areas that indicate their  $1\sigma$  and  $2\sigma$  contours.

It is clear from the figure that the three TF models—as well as NL3—predict a symmetry energy that is simply too stiff to be consistent with such an analysis. However, it appears that systematic uncertainties in the analysis of X-ray bursters continue to hinder the reliable extraction of stellar radii. Indeed, Suleimanov and collaborators have suggested that even the more conservative estimate by Steiner *et al.* must be called into question [54]. The authors of Ref. [54] have proposed a lower limit on the stellar radius of 14 km for neutron stars with masses below  $2.3 M_\odot$ —concluding that neutron-star matter is characterized by a stiff EOS. Adopting this latest constraint, all three of the stiff TF models fit comfortably within it. Thus, at present astrophysical observations are unable to place stringent constraints on either the density dependence of the symmetry energy or the neutron-skin thickness of  $^{208}\text{Pb}$ .

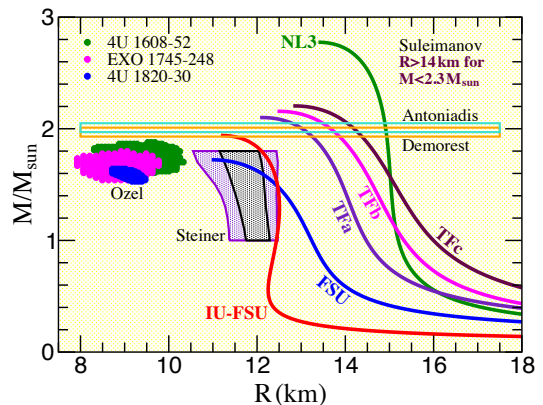


FIG. 4: (Color online) *Mass-vs-Radius* relation predicted by the six models discussed in the text. The horizontal bars in the figure represent two accurate measurements of massive neutron stars as reported in Refs. [48, 49]. The mass-radius constraints suggesting very small stellar radii represent the  $1\sigma$  confidence contours reported in Ref. [51]. The two shaded areas that suggest larger radii are  $1\sigma$  and  $2\sigma$  contours extracted from the analysis of Ref. [53]. Finally, the suggestion of large stellar radii by Suleimanov *et al.* [54] is indicated on the top-right hand side of the figure.

In summary, we have constructed models with large neutron skins to test whether the large central value reported by the PREX collaboration may already be ruled out by existing laboratory or observational data. To do so we have introduced three models with fairly large neutron skins to compute masses, charge radii, centroid energies of monopole resonances, the electric dipole polarizability of  $^{208}\text{Pb}$ , and masses and radii of neutron stars. Based on this set of experimental and observational data, we find no compelling reason to rule out models with large neutron skins. We should mention, however, that the high-resolution measurement of the electric dipole polarizability in  $^{208}\text{Pb}$  places a particularly significant constraint that can only be satisfied at the  $2\sigma$  level. We are confident that improvements in the statistical and systematic accuracy of future measurements of neutron

skins, dipole polarizabilities, and stellar radii will provide vital constraints on the density dependence of the symmetry energy. For now, however, ruling out a thick neutron skin in  $^{208}\text{Pb}$  seems premature.

### Acknowledgments

We would like to thank Profs. Bao-An Li and W. G. Newton for fruitful discussions. This work was supported

in part by grant DE-FD05-92ER40750 from the U.S. Department of Energy, by the National Aeronautics and Space Administration under Grant No. NNX11AC41G issued through the Science Mission Directorate, and the National Science Foundation under Grant No. PHY-1068022.

- 
- [1] S. Abrahamyan, Z. Ahmed, H. Albatineh, K. Aniol, D. Armstrong, et al., Phys. Rev. Lett. **108**, 112502 (2012).
- [2] C. Horowitz, Z. Ahmed, C. Jen, A. Rakhman, P. Souder, et al., Phys. Rev. **C85**, 032501 (2012).
- [3] T. Donnelly, J. Dubach, and I. Sick, Nucl. Phys. **A503**, 589 (1989).
- [4] I. Angeli and K. Marinova, At. Data Nucl. Data Tables **99**, 69 (2013).
- [5] X. Roca-Maza, M. Centelles, X. Viñas, and M. Warda, Phys. Rev. Lett. **106**, 252501 (2011).
- [6] J. Piekarewicz, B. Agrawal, G. Colo, W. Nazarewicz, N. Paar, et al., Phys. Rev. **C85**, 041302 (2012).
- [7] B. A. Brown, Phys. Rev. Lett. **85**, 5296 (2000).
- [8] R. J. Furnstahl, Nucl. Phys. **A706**, 85 (2002).
- [9] M. Centelles, X. Roca-Maza, X. Viñas, and M. Warda, Phys. Rev. Lett. **102**, 122502 (2009).
- [10] M. B. Tsang et al., Phys. Rev. Lett. **92**, 062701 (2004).
- [11] L.-W. Chen, C. M. Ko, and B.-A. Li, Phys. Rev. Lett. **94**, 032701 (2005).
- [12] A. W. Steiner and B.-A. Li, Phys. Rev. **C72**, 041601 (2005).
- [13] D. V. Shetty, S. J. Yennello, and G. A. Souliotis, Phys. Rev. **C76**, 024606 (2007).
- [14] M. B. Tsang et al., Phys. Rev. Lett. **102**, 122701 (2009).
- [15] C. J. Horowitz and J. Piekarewicz, Phys. Rev. Lett. **86**, 5647 (2001).
- [16] C. J. Horowitz and J. Piekarewicz, Phys. Rev. **C64**, 062802 (2001).
- [17] C. J. Horowitz and J. Piekarewicz, Phys. Rev. **C66**, 055803 (2002).
- [18] J. Carriere, C. J. Horowitz, and J. Piekarewicz, Astrophys. J. **593**, 463 (2003).
- [19] A. W. Steiner, M. Prakash, J. M. Lattimer, and P. J. Ellis, Phys. Rept. **411**, 325 (2005).
- [20] B.-A. Li and A. W. Steiner, Phys. Lett. **B642**, 436 (2006).
- [21] J. Piekarewicz, Phys. Rev. **C76**, 064310 (2007).
- [22] M. Tsang et al., Phys. Rev. **C86**, 015803 (2012).
- [23] J. M. Lattimer, Ann. Rev. Nucl. Part. Sci. **62**, 485 (2012).
- [24] A. Carbone, G. Colo, A. Bracco, L.-G. Cao, P. F. Bortignon, et al., Phys. Rev. **C81**, 041301 (2010).
- [25] A. W. Steiner and S. Gandolfi, Phys. Rev. Lett. **108**, 081102 (2012).
- [26] P. Möller, W. D. Myers, H. Sagawa, and S. Yoshida, Phys. Rev. Lett. **108**, 052501 (2012).
- [27] B. G. Todd-Rutel and J. Piekarewicz, Phys. Rev. Lett. **95**, 122501 (2005).
- [28] G. A. Lalazissis, J. König, and P. Ring, Phys. Rev. **C55**, 540 (1997).
- [29] G. A. Lalazissis, S. Raman, and P. Ring, At. Data Nucl. Data Tables **71**, 1 (1999).
- [30] F. J. Fattoyev, C. J. Horowitz, J. Piekarewicz, and G. Shen, Phys. Rev. **C82**, 055803 (2010).
- [31] J. Piekarewicz and M. Centelles, Phys. Rev. **C79**, 054311 (2009).
- [32] G. Audi, A. H. Wapstra, and C. Thibault, Nucl. Phys. **A729**, 337 (2002).
- [33] B. Agrawal, J. De, S. Samaddar, G. Colo, and A. Sulaksono (2013), 1305.5336.
- [34] D. H. Youngblood, H. L. Clark, and Y.-W. Lui, Phys. Rev. Lett. **82**, 691 (1999).
- [35] M. *et al.* Uchida, Phys. Lett. **B557**, 12 (2003).
- [36] M. Uchida, H. Sakaguchi, M. Itoh, M. Yosoi, T. Kawabata, et al., Phys.Rev. **C69**, 051301 (2004).
- [37] T. Li et al., Phys. Rev. Lett. **99**, 162503 (2007).
- [38] T. Li, U. Garg, Y. Liu, R. Marks, B. Nayak, et al., Phys.Rev. **C81**, 034309 (2010).
- [39] U. Garg and D. Patel, *private communication*.
- [40] J. Piekarewicz, Phys. Rev. **C69**, 041301 (2004).
- [41] J. Piekarewicz, Phys. Rev. **C76**, 031301 (2007).
- [42] J. Piekarewicz, J. Phys. **G37**, 064038 (2010).
- [43] A. Tamii et al., Phys. Rev. Lett. **107**, 062502 (2011).
- [44] I. Poltoratska, P. von Neumann-Cosel, A. Tamii, T. Adachi, C. Bertulani, et al., Phys.Rev. **C85**, 041304 (2012).
- [45] P.-G. Reinhard and W. Nazarewicz, Phys. Rev. **C81**, 051303 (2010).
- [46] W. Satula, R. A. Wyss, and M. Rafalski, Phys. Rev. **C74**, 011301 (2006).
- [47] X. Roca-Maza et al., *in preparation*.
- [48] P. B. Demorest, T. Pennucci, S. M. Ransom, M. S. E. Roberts, and J. W. T. Hessels, Nature **467**, 1081 (2010).
- [49] J. Antoniadis, P. C. Freire, N. Wex, T. M. Tauris, R. S. Lynch, et al., Science **340**, 6131 (2013).
- [50] J. M. Lattimer and M. Prakash, Phys. Rept. **442**, 109 (2007).
- [51] F. Özel, G. Baym, and T. Guver, Phys.Rev. **D82**, 101301 (2010).
- [52] F. J. Fattoyev and J. Piekarewicz, Phys. Rev. **C82**, 025805 (2010).
- [53] A. W. Steiner, J. M. Lattimer, and E. F. Brown, Astrophys. J. **722**, 33 (2010).
- [54] V. Suleimanov, J. Poutanen, M. Revnivtsev, and K. Werner, Astrophys.J. **742**, 122 (2011).